Published in final edited form as:
Expert Opin Med Diagn. 2008 September 1; 2(9): 1055–1065. doi:10.1517/17530050802361161.

New imaging techniques in the diagnosis of multiple sclerosis

Yan Fu[1], **Thomas M Talavage**[1,2], and **Ji-Xin Cheng**[1,3]

1 *Purdue University, Weldon School of Biomedical Engineering, West Lafayette, IN 47907, USA*

2 *Purdue University, School of Electrical & Computer Engineering, West Lafayette, IN 47907, USA*

3 *Purdue University, Department of Chemistry, West Lafayette, IN 47907, USA, Tel: + 765 494 4335; Fax: +1765 4% 1912; Email: jcheng@purdue.edu*

Abstract

Background—Multiple sclerosis (MS) is a chronic disabling disorder histopathologically characterized by inflammation, demyelination and axonal loss. Conventional MRI has made most contributions to the diagnosis of MS. However, it is not sufficiently sensitive and specific to reveal the extent and severity of the damage in the disease. Other nuclear magnetic resonance (NMR) techniques including magnetic resonance spectroscopy, magnetization transfer imaging, diffusion weighted and diffusion tensor imaging, and functional MRI have provided additional information that improves the diagnosis and understanding of MS. Optical techniques including optical coherence tomography (OCT) and coherent anti-Stokes Raman scattering (CARS) microscopy have shown promise in diagnosis and mechanistic study of myelin diseases.

Objective—To review new imaging techniques and their potential in diagnosis of MS.

Method—The principles of three imaging techniques (MRI, OCT and CARS) and their applications to MS studies are described. Their advantages and disadvantages are compared.

Conclusion—Conventional MRI remains a critical tool in the diagnosis of MS. Alternative NMR/MRI techniques have improved specificity for the detection of lesions and provided more quantitative information about MS. Optical techniques including OCT and CARS microscopy are opening up new ways for diagnosis and mechanistic study of myelin diseases.

Keywords

coherent anti-Stokes Raman scattering microscopy; magnetic resonance imaging; multiple sclerosis; optical coherence tomography

1. Introduction

Multiple sclerosis (MS) is an autoimmune disease that impairs neurotransmission of the CNS. Focal intensive demyelination and white matter infiltration by lymphocytes and mononuclear cells are pathological hallmarks of the disease [1]. In the absence of therapy repeated attacks lead to an accumulation of MS lesions, which manifests as physical and cognitive disability. MS studies necessitate sensitive and reliable imaging methods for investigating the specific pathological changes of white matter during progression of the disease. MRI is currently the most widely used technique for diagnosis of MS. In conventional MRI, serial T1-weighted imaging allows detection of chronic neurodegeneration [2], with gadolinium-enhanced contrast depicting not only immune cell migration across the blood-brain barrier but also active

Correspondence to: Ji-Xin Cheng.

inflammation in lesions [3]. Serial T2-weighted imaging is more widely used to identify the number and volume of clinically silent lesions. These MRI acquisition techniques have greatly facilitated clinical observation and understanding of MS, and diagnostic criteria based on the MRI findings have been proposed [4]. However, conventional MRI shows insufficient sensitivity and specificity to indicate the extent and severity of highly diverse MS lesions. The correlation between lesion quantification by MRI and functional disabilities as assessed by clinical measures is also poor.

During the past decade, numerous other nuclear magnetic resonance (NMR) techniques have been developed or exploited to improve the sensitivity and specificity in the detection of MS lesions. These additional NMR techniques – including magnetic resonance spectroscopy (MRS), magnetization transfer imaging (MTI), diffusion weighted and diffusion tensor imaging (DWI and DTI), and functional MRI (fMRI) – have helped us better understand the pathologic processes within and outside the lesions [5].

Moreover, new optical imaging techniques including optical coherence tomography (OCT) [6] and coherent anti-Stokes Raman scattering (CARS) microscopy [7,8] permit potentially cheaper and faster diagnosis of MS. OCT scans measure axonal loss and damage associated with optic neuritis in MS [9], with a good correlation between the reductions of the retinal thickness/macular volume and the clinical measures of disability. CARS microscopy allows label-free imaging of myelin with sub micron 3D resolution [10] and has been used to monitor lyso-PtdCho-induced demyelination in real time [11].

The following sections review the technology principle of each imaging method and their applications to MS study. Advantages and limitations are compared in the end.

2. Magnetic resonance imaging

2.1 Technology principle

NMR techniques, including MRI, exploit resonance and relaxation properties of the protons in nuclei having an odd number of nucleons. Each proton has charge and quantum spin (effectively angular momentum), resulting in each proton also having a magnetic dipole moment. In MRI the body is placed in an external magnetic field thousands of times stronger than that of the Earth, leading to the protons in the body (and their associated magnetic moments) aligning either parallel or antiparallel to the applied field. The aligned protons are then perturbed by radiofrequency waves (pulses) that cause a proportion of protons to (coherently) change their alignment, producing a net magnetic moment that is oriented at an arbitrary angle relative to the applied field. This net magnetic moment (and associated net angular momentum) subsequently precesses about the applied magnetic field. When the radiofrequency waves are turned off, the precessing protons will return (relax) to their previously aligned states, inducing a (decaying) signal in local radiofrequency coils that can be measured and used to create magnetic resonance images that vary depending on the tissue being scanned.

The longitudinal relaxation time (T1, time to return to thermal equilibrium) and the transverse relaxation time (T2, time to loss of coherence for the precessing net magnetic moment) are two important parameters in MRI for characterization of MS lesions. By altering the strength, orientation, and timing of radiofrequency pulse sequences, T1 and T2 relaxation times can be highlighted. Image contrast comes from differences between tissues with intrinsically different proton densities which can be either T1 or T2 weighted in order to emphasize the differences between normal and pathological diseases.

2.2 Conventional magnetic resonance imaging

Hydrogen protons of water are highly abundant in our body and consequently they are used in MRI to visualize edema, inflammation, demyelination and axonal damage in MS lesions. In T1 -weighted images, MS lesions show lower signal than the surrounding white matter, suggestive of acute edema or tissue disruption [12]. Chronic T1 hypointensity, referred to as 'black holes', represents the most severe and chronic stage of MS lesions characterized pathologically by irreversible axonal loss, demyelination and extracellular edema [12,13]. In T1-weighted imaging, the lesions in their earliest stage can be robustly visualized with gadolinium-based contrast agents. Gadolinium is normally excluded from the brain by the blood-brain barrier. The gadolinium labeling, usually persisting for 2 – 6 weeks [14], corresponds pathologically to early active areas of inflammation and blood–brain barrier dysfunction [3]. In T2-weighted images, MS lesions appear as bright areas against a gray or more neutral background. The T2 hyperintense lesions represent any of the tissue changes including edema, inflammation, demyelination, axonal loss and gliosis. Once detected, a lesion typically persists in the T2 hyperintense stage for many years. The sensitivity of T2-weighted imaging can be further increased by a technique called fluid-attenuated inversion recovery (FLAIR), which is used for detection of subcortical and periventricular lesions by suppressing the T2 signal from cerebrospinal fluid [15].

Conventional MRI has become a critical tool in the diagnosis of MS. Contrast-enhanced MRI has served as a standard among the diagnostic criteria for MS, primarily serving as a tool for the determination of the dissemination in space and dissemination in time of lesions [16]. Diagnostic criteria also involve T2-weighted imaging, primarily in a follow-up capacity, with T2-weighteti FLAIR imaging, whether performed using a two-dimensional (slice) acquisition or a three-dimensional (slab) acquisition, now serving as the primary mechanism of identification of MS lesions [17]. In fact T2-weighted imaging has been so successful in demonstrating specificity and sensitivity for clinically definite MS that it has been proposed that contrast-enhanced MRI may not be necessary for effective identification of clinically definite MS [18] (see also [19]).

3. Other nuclear magnetic resonance techniques

Although conventional MRI based on T1- and T2-weighed contrasts has become an important paraclinical tool for diagnosis of MS [4], this method does not provide: i) sufficient sensitivity to make an initial diagnosis as early as possible in order to slow down the disease progression; ii) sufficient specificity to predict the severity of the disease; and iii) good correlation between abnormalities in magnetic resonance images and clinical evolution of disease to determine the therapy strategy. In order to achieve greater diagnostic value from MRI, and to provide more information about the nature and the extent of tissue damage, alternative NMR techniques have been applied of developed [20–24], as summarized below.

3.1 Magnetic resonance spectroscopy

Proton MRS offers a non invasive way to observe biochemical changes during the pathological processes in MS [25]. An MR spectrum in a small volume of tissue displays multiple peaks or resonances representing cellular metabolic by-products including lipids, lactic acid, *N*-acetyl aspartate (NAA), glutamate/glutamine, creatine, choline and myo-inositol [26,27], for example, using point-resolved spectroscopy (PRESS) with echo times (TE) of 35 ms, repetition time (TR) of 1.5 s and a voxel size of 8 cm^3. The sharpness and height of a given peak are governed not only by a molecule's identity and concentration but also by its mobility [28]. Only free mobile molecules produce well defined resonances. Changes of height or area of peaks from the metabolites, in comparison with creatine which remains relatively constant despite pathology, illustrate abnormalities in the brain tissue.

Among the various compounds detectable using proton MRS, the NAA resonance contributes to the most prominent signal from the adult human brain and is generally the most informative spectral feature in the detection of brain lesions. NAA is an amino acid derivative normally confined to axons and neurons [29]. Reduced NAA correlates with axonal injury or loss [30], found not only with acute and chronic MS lesions but also in the normal appearing white matter of relapsing–remitting, secondary progressive, and primary progressive MS patients [31,32]. Moreover, the degree of reduction has repeatedly been found to correlate with the degree of clinical disability [33–35]. Additionally, NAA levels in the whole brain can also be measured. Studies have shown that the variations of global NAA level in healthy controls were small (< 5%; $p < 0.01$) [36,37], whereas whole brain NAA declined linearly with increasing MS disease duration. Moreover, the rate of decline for NAA measured by MRS was 3.6 times faster than the global brain atrophy estimated by MRI [38]. Therefore, the whole brain NAA measured by MRS appears to be a more sensitive neuroimaging marker of disease progression.

In addition to NAA, other spectral peaks related to metabolites have been found to be informative of the health of the tissue in the brain. Promising results have been obtained with regard to using choline and myo-inositol as markers for measuring or detecting sustained damage to non-neuronal cells within the brain [39].

Based on the success of measuring NAA, choline, and myo-inositol with proton MRS, it has become desirable to add this imaging technique to the clinical diagnostic battery. However, MRS is highly sensitive to imaging parameters and pulse sequences, with different echo times being preferred for the measurement of different compounds (e.g., a longer echo time will produce greater sensitivity to NAA but lesser sensitivity to myo-inositol). Therefore, a set of standardized guidelines has recently been proposed [40] to increase the potential for proton MRS to become a standard MS detection and tracking technique.

3.2 Magnetization transfer imaging

Although protons associated with macromolecules are difficult to be captured by MRI, interactions between these bound protons and adjacent free water molecules result in a continuous exchange of magnetization, which can be measured as magnetization transfer [41]. Magnetization transfer contrast reflects the concentration of macromolecular protons. A quantitative measurement of this effect, termed the magnetization transfer ratio (MTR), is obtained by means of selective saturation of the bound magnetization pool and measurement of the resultant decrease in water signal intensity due to transfer of this saturation in regions undergoing exchange [42]. A marked reduction of MTR values in MS lesions was suggested to indicate severe tissue damage, primarily associated with demyelination [43], although the effects of edema and changes in other macro-molecules also contribute to changes in MTR [44]. Focal changes in magnetization transfer precede the appearance of gadolinium-enhancing lesions and T2-weighted MRI lesions [45,46], suggesting that MTI may offer increased sensitivity and specificity for studies of MS disease [47]. The future work will focus on long-term longitudinal studies to determine the predictive value of MTR in MS.

3.3 Diffusion weighted imaging and diffusion tensor imaging

DWI and DTI provide information about the orientation, size, integrity and geometry of tissue fibers by measuring the motion of tissue water [48]. Water molecules in highly organized tissue, such as white matter, have diminished mobility. As a result, their apparent diffusion coefficient (ADC) is lower than in free water. Tissue damage in MS results in abnormal water motion, thus modifying the ADC values that are observed in DWI. DTI acquires multiple diffusion weighted images with different orientations and thereby measures diffusion anisotropies [49]. By quantifying anisotropy, DTI allows detection of pathological change in white matter tracts, including demyelination and loss of axons [50]. Besides identification of severe tissue damage,

DTI is also sensitive to subtle changes in the normal appearing white matter [51]. Studies of lesions in different subtypes of MS show significant correlations between DTI findings and MS clinical disability [52–54]. In addition, DTI allows performance of 'fiber tracking', which is able to generate three-dimensional images of selected axonal tracts. Fiber tracking can be used to investigate individual functional pathways within the brain or cervical spinal cord and evaluate their remote response to a demyelinating lesion [55,56].

Because DTI allows encoding properties varying with space, shape and orientation of axonal fibers, DTI has the potential to decode these properties and therefore differentiate the origin of tissue damage (only myelin or both myelin and axonal injury occurs) [50], In the future, systematic studies are needed to examine the reproducibility of DWI and DTI findings and long-term longitudinal studies are required to determine the value of DTI measurements in MS.

3.4 Functional magnetic resonance imaging

fMRI is an indirect measure of neural activities during motor, sensory, and cognitive tasks. It can be used to identify changes in brain activation associated with disease, fMRI detects areas of the brain that have changes in the relationship between blood flow and local oxygen consumption through the blood oxygenation level-dependent effect [57]. fMRI signals most likely reflect changes in local synaptic activity during task performance compared with rest. Unlike other techniques mentioned above, fMRI is not yet used clinically for the diagnosis of MS. Rather it has been used in research settings to examine the functional reorganization as a consequence of demyelination and tissue loss in MS. The functional reorganization may serve as an adaptive response to compensate clinical disability [58,59]. Long-term longitudinal studies are needed to examine the correlation between fMRI activity and other magnetic resonance measurements, as well as clinical measures of disease activity and progression [60].

3.5 Summary of nuclear magnetic resonance techniques

A comparison of various NMR techniques is shown in Table 1. Conventional MRI remains the major clinical tool for the diagnosis of MS. Alternative/advanced NMR/MRI techniques have improved sensitivity and specificity for the detection of lesions and provided more quantitative information to extend our understanding of MS processes. Conversely, these techniques have yet to demonstrate greater sensitivity to the detection of MS than conventional MRI, leaving this an open area of investigation. Meanwhile, advances in biomedical optics have opened up new possibilities for MS diagnosis. Two promising optical techniques are reviewed below.

4. Optical coherence tomography

4.1 Technology principle

OCT is a noninvasive, noncontact, transpupillary imaging technique used for imaging retinal structures *in vivo*. By using an interferometer in conjunction with a low-coherence light source, OCT detects light reflections within a tissue and provides cross-sectional images [61]. The spectacular advances in OCT allow differentiation of major retinal layers and analysis of tissue thickness and volume with a resolution of about 3 μm with high-resolution OCT [62].

4.2 Application of optical coherence tomography to the study of multiple sclerosis

Because the retina and optic nerve are often affected by MS, OCT is an ideal technique to assess the impact of MS on the retina by measuring the retinal nerve fiber layer (RNFL) thickness and macular volume. The reductions of RNFL thickness and macular volume are associated with axonal loss and secondary retinal ganglion cell loss, respectively. Trip and

colleagues [9] studied 25 patients with optic neuritis and 15 controls by OCT. The result showed that the RNFL thickness was reduced by 33% ($p < 0.001$) and the macular volume was reduced by 11% ($p < 0.001$) in patients with optic neuritis compared with healthy people. When the affected eye was compared with the unaffected eye in the patients, the RNFL thickness was reduced by 27% ($p < 0.001$) and macular volume by 9% ($p < 0.001$). This result was in agreement with studies from other groups [63–65]. OCT measurements were also found to correlate with visual dysfunction [6], These studies suggest that OCT can provide valid, reliable and reproducible data to track neurodegeneration within the retina of MS patients with optical neuropathy.

Recently, Pulicken *et al*. [66] investigated axonal damage in subtypes of MS with OCT. Progressive MS cases showed more marked decreases in RNFL thickness and macular volume than relapsing–remitting MS. Further, through comparison of OCT measurements with MRI of brain atrophy, the authors found that RNFL thickness was associated with brain parenchymal fraction in MS, an index of brain atrophy [67]. These data suggest that quantification of RNFL thickness in the retina by OCT provides concurrent information about MRI of brain abnormality in MS. Future work will focus on the examination of OCT in longitudinal studies as a potential biomarker of retinal pathology in MS and an outcome measure of the neuroprotective effects of new treatments.

5. Coherent anti-Stokes Raman scattering (CARS) imaging

5.1 Technology principle

CARS is a four-wave mixing process in which three laser fields at the pump $(\omega)_p$), Stokes (ω_s), and probe (ω'_p) frequencies interact with a medium to generate a new field at the anti-Stokes frequency $\omega_{as} = (\omega_p - \omega_s) + \omega'_p$. In most experiments, the pump field Ep and probe field E′p come from the same laser beam. The CARS signal arises from any medium with nonzero third-order susceptibility $\chi^{(3)}$. When the beating frequency ($'_p - -_s$) is in resonance with a molecular vibration, the mixed pump and Stokes fields can effectively excite the molecule to a vibrational state [68]. Therefore, molecules in resonance produce larger signal than those off resonance, providing vibrational contrast in a CARS image. CARS microscopy offers the following advantages [7,8].

5.1.1 Chemical selectivity—Because the contrast in CARS microscopy arises from intrinsic molecular vibrations, it is able to produce images with chemically selective contrasts when the laser frequency difference ($\omega_p - \omega_s$) is tuned to different Raman bands. For example, CARS microscopy has been used to probe lipid when $\omega_p - \omega_s$ was tuned to CH_2 stretching vibrational mode at 2840 cm^{-1} [69], water when $\omega_p - \omega_s$ to OH stretching mode at 3300 cm^{-1} [70]. For weak Raman bands, however, the chemical selectivity of CARS microscopy is limited due to the existence of a nonresonant background that arises from the electronic contribution to $\chi^{(3)}$. This nonresonant background is coherently mixed with the vibrationally resonant signal, which limits the sensitivity of CARS in detecting weak Raman bands. Additionally, the resonant CARS signal decreases quadratically with the molecular concentration and can be buried in the nonresonant background contributed by the solvent. In CARS microscopy, near-infrared laser excitation avoids two-photon electronic enhancement of the nonresonant background [71] and picosecond pulse excitation further improves the signal to background ratio [72]. As reviewed in [7], a number of advanced strategies have been used to reduce the nonresonant background.

5.1.2 High detection sensitivity—As a coherent process, the CARS fields from different molecules have a well defined phase relationship. Coherent addition of the CARS fields results in a directional signal, which greatly facilitates the signal collection. The coherent addition also results in a quadratic signal increase with respect to the density of molecular oscillators,

versus the linear increase of spontaneous Raman signal. For a bulk liquid, the CARS signal can be larger than the spontaneous Raman signal by nine orders of magnitude [68]. Moreover, by using picosecond pulses to match the width of most Raman lines, the pulse energy is focused on a single Raman band [72]. With picosecond laser excitations, Li *et al*. [69] have shown that CARS microscopy was able to probe 10% dipalmitoyl phosphatidylcholine with fully deuterated acyl chains (d62-DPPC) in a single bilayer, which corresponded to 2×10^4 DPPC molecules inside the focal area of $(0.25\ \mu m)^2$. Picosecond pulse excitation can be realized by using two synchronized Ti-sapphire lasers [72] or using an optical parametric oscillator pumped by a pulsed laser [73,74].

5.1.3 High imaging speed—The large signal level in CARS microscopy enables high speed imaging which is important for live cell and tissue studies. In laser-scanning microscopy with high repetition rate (in MHz) lasers, an image acquisition speed at one frame per second has been achieved [75], and has been recently increased to 20 frames per second [76]. The high imaging speed not only avoids respiration-induced image distortion during *in vivo* imaging [76,77] but also allows real-time inspection of demyelination in live tissues [11].

5.1.4 Submicron three-dimensional resolution—The nonlinear optical excitation ensures that the signal is only generated at the center of the focus, offering CARS microscopy inherent three-dimensional spatial resolution. The lateral and axial resolutions with a 60 × water immersion objective were measured to be 0.75 and 0.23 μm [75], which allows detection of subcellular structures in a tissue environment.

5.2 Applications to the study of myelin sheath

Demyelination is a known pathological hallmark of MS. However, MR techniques are unable to detect nonaqueous protons in myelin because i) the MR signal decays to zero in a few tens of microseconds; and ii) the MR signal from lipids and proteins in myelin is indistinguishable from other nonaqueous constituents in CNS [78]. This difficulty can be nicely compensated by CARS microscopy which is naturally sensitive to molecular assemblies such as lipid membranes. In the CNS, myelin is a lamellar membranous structure consisting of 70% lipid and 30% protein by weight [79]. The high density of CH_2 groups in lipid leads to a large CARS signal arising from the CH_2 stretching vibrational mode at 2840 cm^{-1}. CARS microscopy has been applied to imaging of intact myelin and demyelination in *ex vivo* tissues and live animals, as summarized below.

5.2.1 Vibrational imaging of myelin with submicron three-dimensional resolution—The CARS signal from the intrinsic CH_2 vibrations permits nondestructive imaging of myelin under physiological conditions. This advantage makes CARS microscopy superior to other myelin imaging techniques. Presently, the major high-resolution tools used for myelin observation in the postmortem setting are electron microscopy and light microscopy. Although electron microscopy has provided plenty of ultra-structural information of cellular morphology in MS lesions, the complicated sample preparation (e.g., fixation and dehydration) could perturb axonal structure and complicate data analysis. Demyelination lesions can also be identified by optical microscopy using luxol-fast blue [80] or lipophilic dye [81] staining. Nevertheless, the nonspecific binding and inefficient diffusion of dyes obscure the data analysis. With label-free vibrational imaging, CARS microscopy overcomes these limitations and provides the capability of observing intact myelin in *ex vivo* tissues and live animals. Typical CARS images of myelinated axons in white matter of guinea-pig spinal cord and brain are shown in Figure 1A and B, respectively. The myelin wrapping parallel axons displays a high contrast, with a resonant signal to nonresonant background ratio of 10:1 [10]. The three-dimensional submicron resolution allows observation of specific myelin structure at a node of Ranvier (Figure 1C). Three-dimensional images of myelin structure can be reconstructed to

show the tubular myelin sheath wrapping the axons in the spinal cord (Figure 1D), Meanwhile, Z stacks of CARS images of myelin provide spatial information of brain myelin fibers. For example, Figure 1E shows the high density of axons with random orientations in brain cortex and Figure 1F shows tightly packed fiber bundles in the corpus callosum.

5.2.2 Multimodal nonlinear optical imaging of CNS on a CARS microscope— Multimodality is important in nonlinear optical imaging study of CNS because each modality has its own distinctive advantages: two-photon excited fluorescence (TPEF) can be used to visualize proteins, ions with fluorescent labeling or specific autofluorescent structures; sum-frequency generation (SFG) is selective to non-centrosymmetric molecular assemblies such as collagen fibrils; and CARS is naturally sensitive to myelin. By combination of TPEF, SFG and CARS on the same microscope platform, Fu *et al.* [82] demonstrated multimodal nonlinear optical imaging of CNS by CARS imaging of myelin sheath, SFG imaging of astrocyte processes, and TPEF imaging of calcium indicators in the same spinal tissue. This approach can be used to monitor multiple events during myelin disruption.

5.2.3 *In vivo* CARS imaging of nerve fibers—CARS microscopy offers two advantages for *in vivo* imaging. First, the capability of label-free imaging of myelin is particularly important for *in vivo* studies in which the labeling is complicated by inefficient diffusion and non-specific binding in the tissue environment. Second, the CARS signal can be epi-detected (i.e., in the backward direction), which is important for imaging live animals because the forward CARS signal cannot pass through a thick tissue [76,77]. By using minimal surgery to cut open the skin, Huff and Cheng |77] demonstrated *in vivo* CARS imaging of sciatic nerve and surrounding adipocytes [77], The epi-detected CARS signals from the sciatic nerve were found to arise from interfaces as well as back reflection of forward CARS signal. Notably, a miniature objective lens has been used for *in situ* imaging of rat spinal cord with minimal surgery to the vertebra [83].

5.2.4 Real-time CARS imaging of demyelination process—The high data acquisition speed in CARS microscopy allowed real-time imaging of lyso-PtdCho-induced myelin degradation. Through CARS imaging of *ex vivo* guinea pig spinal tissues and *in vivo* mouse sciatic nerves, lyso-PtdCho has been shown to cause acute myelin swelling (Figure 2A and B), The swollen myelin displays decreased CARS intensity (intensity profiles below Figure 2A and B), consistent with myelin vesiculation observed by EM. Combining real-time CARS imaging and electrophysiological recording, a pathway that involves Ca^{2+} influx into myelin and subsequent calpain and $cPLA_2$ activation was revealed [11].

In summary, the above studies demonstrated that CARS microscopy is a unique tool for myelin study. The future work will focus on the systematic characterization of lesions in MS patient's spinal cord and brain with high sensitivity and specificity. The mechanism of myelin damage in different stages, especially in the early stage, will be explored. CARS microscopy has not yet been applied to the detection of MS lesions *in vivo.* However, current studies of demyelination in *ex vivo* tissues and live animals have shown the potential of this technique in studies of myelin diseases.

6. Conclusions

MRI is an established technique for diagnosis of MS. Advanced magnetic resonance techniques have improved the detection of the extent and severity of the disease. OCT provides good correlation between reduced retinal nerve fiber layer thickness and neuronal degeneration in MS patients. Based on C–H vibration resonance, CARS microscopy allows real-time imaging of intact myelin and demyelination with submicron three-dimensional resolution. These

advanced neuroimaging techniques promise to detect MS in the early stages and provide new possibilities for understanding MS pathogenesis.

7. Expert opinion

The contrast mechanisms and major parameters of three MS imaging techniques – MRI, OCT and CARS microscopy – are compared in Table 2. Based on ^{1}H nuclei magnetic resonance of water molecules, MRI allows reliable observation of MS lesions *in vivo* and is currently the most important neuroimaging tool for diagnosis of MS. The recent advances in MR techniques have improved pathological specificity and sensitivity in the detection of MS lesions. However, the clinical correlation of MRI is still limited by its relatively low spatial resolution. To help the translation of imaging measurement into treatment, there is an urgent need for improving the resolution of MRI to correlate different types of cellular damage with clinical status.

Utilizing back reflection of low-coherence photons, OCT is able to provide accurate and quantitative measurements of axonal loss in retina. OCT measurements have concluded the association between severe visual dysfunction and pathology in the retina of MS patients, suggesting that OCT holds promise as a biomarker for neurodegeneration in MS. However, the retina and optic nerve represent a discrete system in the CNS and axonal degeneration is a specific pathological process contributing to the irrecoverable deficit and developing later in the course of the disease [33]. Therefore, correlation of OCT measurements of retina to the pathological changes occurring within the CNS has to be validated through studies in a larger population and a longer course.

By capturing the resonance from C–H vibration in membrane lipid, CARS microscopy allows molecular imaging of myelin with three-dimensional submicron resolution, CARS microscopy has been used to identify myelin degeneration and reveal the molecular pathways in lyso-PtdCho induced demyelination model [11]. *In vivo* CARS imaging of mouse sciatic nerve has been accomplished with the aid of minimally invasive surgery [77]. A miniature objective lens with a tip diameter of 1.3 mm, namely the MicroProbe objective, has been used for CARS imaging of spinal cord white matter in an euthanized rat [83]. These applications and technical advances demonstrate CARS imaging as a promising tool for the study of MS in the postmortem setting. For noninvasive diagnosis of MS, new technical developments are needed to overcome the limited optical penetration depth. One possibility is to probe the myelin sheath in optic nerves with epi-detected CARS using an ophthalmoscope mode. With distinct specificity and sufficient sensitivity to myelin, CARS microscopy has the potential to identify the early status of MS and also differentiate the different types of MS lesions based on myelin changes.

In summary, MRI, OCT and CARS microscopy each hold their own strength in the study of MS. MRI provides information about the entire pathologic range of disease through scanning the whole brain. OCT provides accurate and meaningful measures of axonal damage in the retina. CARS microscopy directly visualizes myelin damage in CNS tissues with submicron spatial resolution. As for data interpretation, specific expertise is still need for all three techniques. Although OCT and CARS microscopy offer a potentially cost-effective way for diagnosis of MS compared with MRI, their studies have been restricted in the laboratories so far. With further development of these two techniques, we expect that their advantages would be utilized under clinical settings. Finally, in the absence of one ultimate neuroimaging tool that can fulfill all the requisites in the study of MS, a combination of complementary knowledge obtained from different modalities will be a wise choice.

Acknowledgements

Declaration of interest

This work was supported by NIH grant R01 EB007243 to Ji-Xin Cheng.

Bibliography

1. Compston A, Coles A. Multiple sclerosis. Lancet 2002;359:1221–31. [PubMed: 11955556]
2. Bagnato F, Jeffries N, Richert ND, et al. Evolution of T1 black holes in patients with multiple sclerosis imaged monthly for 4 years. Brain 2003;126:1782–9. [PubMed: 12821527]
3. Brück W, Bitsch A, Kolenda H, et al. Inflammatory central nervous system demyelination: correlation of magnetic resonance imaging findings with lesion pathology. Ann Neurol 1997;42:783–93. [PubMed: 9392578]
4. McDonald WI, Compston A, Edan G, et al. Recommended diagnostic criteria for multiple sclerosis: guidelines from the international panel on the diagnosis of multiple sclerosis. Ann Neurol 2001;50:121–7. [PubMed: 11456302]
5. Filippi M, Grossman RI. MRI techniques to monitor MS evolution: the present and the future. Neurology 2002;58:1147–53. [PubMed: 11971079]
6. Kallenbach K, Frederiksen J. Optical coherence tomography in optic neuritis and multiple sclerosis: a review. Eur J Neurol 2007;14:841–9. [PubMed: 17662003]
7. Cheng JX. Coherent anti-Stokes Raman scattering microscopy. Appl Spectrosc 2007;61:A197–208.
8. Cheng JX, Xie XS. Coherent anti-Stokes Raman scattering microscopy: instrumentation, theory, and applications. J Phys Chem B 2004;108:827–40.
9. Trip SA, Schlottmann PG, Jones SJ, et al. Retinal nerve fiber layer axonal loss and visual dysfunction in optic neuritis. Ann Neurol 2005;58:383–91. [PubMed: 16075460]
10. Wang H, Fu Y, Zickmund P, et al. Coherent anti-Stokes Raman scattering imaging of live spinal tissues. Biophys J 2005;89:581–91. [PubMed: 15834003]
11. Fu Y, Wang H, Huff TB, et al. Coherent anti-Stokes Raman scattering imaging of myelin degradation reveals a calcium dependent pathway in lyso-PtdCho induced demyelination. J Neurosci Res 2007;85:2870–81. [PubMed: 17551984]
12. Van Walderveen MAA, Kamphorst W, Scheltens P, et al. Histopathologic correlate of hypointense lesions on T1-weighted spin-echo MRI in multiple sclerosis. Neurology 1998;50:1282–8. [PubMed: 9595975]
13. Brex PA, Parker GJM, Leary SM, et al. Lesion heterogeneity in multiple slcerosis: a study of the relations between appearances on T1 weighted images, T1 relaxation times, and metabolite concentrations. J Neurol Neurosurg Psychiatry 2000;68:627–32. [PubMed: 10766895]
14. Lai M, Hodgson T, Gawne-Cain M, et al. A preliminary study into the sensitivity of disease activity detection by serial weekly magnetic resonance imaging in multiple sclerosis. J Neurol Neurosurg Psychiatry 1996;60:339–41. [PubMed: 8609517]
15. Bakshi R, Ariyaratana S, Benedict RHB, Jacobs L. Fluid-attenuated inversion recovery magnetic resonance imaging detects cortical and juxtacortical multiple sclerosis lesions. Arch Neurol 2001;58:742–8. [PubMed: 11346369]
16. Polman CH, Reingold SC, Edan G, et al. Diagnostic criteria for multiple sclerosis: 2005 revisions to the ‘McDonald Criteria’. Ann Neurol 2005;58:840–6. [PubMed: 16283615]
17. Bink A, Schmitt M, Gaa J, et al. Detection of lesions in multiple sclerosis by 2D FLAIR and single-slab 3D FLAIR sequences at 3.0 T: initial results. Eur Radiol 2006;16:1104–10. [PubMed: 16425026]
18. Swanton JK, Fernando K, Dalton CM, et al. Modification of MRI criteria for multiple sclerosis in patients with clinically isolated syndromes. J Neurol Neurosurg Psychiatry 2006;77:830–3. [PubMed: 16043456]
19. Rovira A, León A. MR in the diagnosis and monitoring of multiple sclerosis: an overview. Eur J Radiol. 2008published online 21 April 2008
20. Arnold DL, Matthews PM. MRI in the diagnosis and management of multiple sclerosis. Neurology 2002;58:S23–31. [PubMed: 11971123]
21. Zivadinov R. Can imaging techniques measure neuroprotection and remyelination in multiple sclerosis? Neurology 2007;68:S72–82. [PubMed: 17548573]
22. Traboulsee A, Zhao G, Li DKB. Neuroimaging in multiple sclerosis. Neurol Clin 2005;23:131–48. [PubMed: 15661091]

23. Rooney WD, Coyle PK. Recent advances in the neuroimaging of multiple sclerosis. Curr Neurol Neurosci Rep 2005;5:217–24. [PubMed: 15865887]
24. Joy, JE.; Richard, B.; Johnston, J. Multiple sclerosis: current status and strategies for the future. Washington, DC: National Academy Press; 2001.
25. Richards TL. Proton MR spectroscopy in multiple sclerosis: value in establishing diagnosis, monitoring progression, and evaluating therapy. AJR Am J Roentgenol 1991;157:1073–8. [PubMed: 1927795]
26. Arús C, Chang Y, Bárány M. Proton nuclear magnetic resonance spectra of excised rat brain. Assignment of resonances. Physiol Chem Phys Med NMR 1985;17:23–33. [PubMed: 4034678]
27. Lin A, Ross BD, Harris K, Wong W. Efficacy of proton magnetic resonance spectroscopy in neurological diagnosis and neurotherapeutic decision making. NeuroRx 2005;2:197–214. [PubMed: 15897945]
28. Matthews PM, de Stefano N, Narayanan S, et al. Putting magnetic resonance spectroscopy studies in context: axonal damage and disability in multiple sclerosis. Semin Neurol 1998;18:327–36. [PubMed: 9817537]
29. Simmons ML, Frondoza CG, Coyle JT. Immunocytochemical localization of N-acetyl-aspartate with monoclonal antibodies. Neuroscience 1991;45:37–45. [PubMed: 1754068]
30. Wolinsky JS, Narayanan S. Magnetic resonance spectroscopy in multiple sclerosis: window into the diseased brain. Curr Opin Neurol 2002;15:247–51. [PubMed: 12045720]
31. Arnold DL, de Stefano N, Matthews PM, Trapp BD. N-acetylaspartare: usefulness as an indicator of viable neuronal tissue. Ann Neural 2001;50:823–5.
32. Narayanan S. Magnetic resonance spectroscopy in the monitoring of multiple sclerosis. J Neuroimaging 2005;15:S46–57.
33. Davie CA, Barker GJ, Webb S, et al. Persistent functional deficit in multiple sclerosis and autosomal dominant cerebellar ataxia is associated with axon loss. Brain 1996;118:1583–92. [PubMed: 8595487]
34. De Stefano N, Narayanan S, Francis GS, et al. Evidence of axonal damage in the early stages of multiple sclerosis and its relevance to disability. Arch Neurol 2001;58:65–70. [PubMed: 11176938]
35. Lee MA, Blamire AM, Pendlebury S, et al. Axonal injury or loss in the internal capsule and motor impairment in multiple sclerosis. Arch Neurol 2000;57:65–70. [PubMed: 10634450]
36. Gonen O, Catalaa I, Babb JS, et al. Total brain N-acetylaspartate: a new measure of disease load in MS. Neurology 2000;54:15–9. [PubMed: 10636119]
37. Gonen O, Viswanathan AK, Catalaa I, et al. Total brain N-acetylaspartate concentration in normal, age-grouped females: quantitation with non-echo proton NMR spectroscopy. Magn Resort Med 1998;40:684–9.
38. Ge Y, Gonen O, Inglese M, et al. Neuronal cell injury precedes brain atrophy in multiple sclerosis. Neurology 2004;62:624–7. [PubMed: 14981182]
39. Chard DT, Griffin CM, McLean MA, et al. Brain metabolite changes in cortical grey and normal-appearing white matter in clinically early relapsing-remitting multiple sclerosis. Brain 2002;125:2342–52. [PubMed: 12244090]
40. De Stefano N, Filippi M, Miller D, et al. Guidelines for using proton MR spectroscopy in multicenter clinical MS studies. Neurology 2007;69:942–52.
41. Wolff S, Balaban RS. Magnetization transfer contrast (MTC) and tissue water proton relaxation in vivo. Magn Reson Med 1998;10:135–44. [PubMed: 2547135]
42. Henkelman RM, Huang XM, Xiang QS, et al. Quantitative interpretation of magnetization transfer. Magn Reson Med 1993;29:759–66. [PubMed: 8350718]
43. Schmierer K, Scaravilli F, Altmann DR, et al. Magnetization transfer ratio and myelin in postmortem multiple sclerosis brain. Ann Neurol 2004;56:407–15. [PubMed: 15349868]
44. Dousset V, Grossman RI, Ramer KN, et al. Experimental allergic encephalomyelitis and multiple sclerosis: lesion characterization with magnetization transfer imaging. Radiology 1992;182:483–91. [PubMed: 1732968]

45. Filippi M, Rocca MA, Martino G, et al. Magnetization transfer changes in the normal appearing white matter precede the appearance of enhancing lesions in patients with multiple sclerosis. Ann Neurol 1998;43:809–14. [PubMed: 9629851]
46. Pike GB, De Stefano N, Narayanan S, et al. Multiple sclerosis: magnetization transfer MR imaging of white matter before lesion appearance onT2-weighted images. Neuroradiology 2000;215:824–30.
47. Filippi M, Rocca MA. Magnetization transfer magnetic resonance imaging in the assessment of neurological diseases. J Neuroimaging 2004;14:303–13. [PubMed: 15358949]
48. Rovaris M, Gass A, Bammer R, et al. Diffusion MRI in multiple sclerosis. Neurology 2005;65:1526–32. [PubMed: 16301477]
49. Alexander AL, Lee JE, Lazar M, Field AS. Diffusion tensor imaging of the brain. Neurotherapeutics 2007;4:316–29. [PubMed: 17599699]
50. Ge Y, Law M, Grossman RI. Application of diffusion tensor MR imaging in multiple sclerosis. Ann NY Acad Sci 2005;1064:202–19. [PubMed: 16394158]
51. Filippi M, Cercignani M, Inglese M, et al. Diffusion tensor magnetic resonance imaging in multiple sclerosis. Neurology 2001;56:304–11. [PubMed: 11171893]
52. Nusbaum AO, Tang CY, Wei TC, et al. Whole-brain diffusion MR histograms differ between MS subtypes. Neurology 2000;54:1421–7. [PubMed: 10751250]
53. Cercignani M, Inglese M, Pagani E, et al. Mean diffusivity and fractional anisotropy histograms of patients with multiple sclerosis. AJNR Am J Neuroradiol 2001;22:952–8. [PubMed: 11337342]
54. Castrita Scanderbeg A, Tomaiuolo F, Sabatini U, et al. Demyelinating plaques in relapsing-remitting and secondary-progressive multiple sclerosis: assessment with diffusion MR imaging. AJNR Am J Neuroradiol 2000;21:862–8. [PubMed: 10815661]
55. Ciccarelli O, Toosy AT, Hickman SJ, et al. Optic radiation changes after optic neuritis detected by tractography-based group mapping. Hum Brain Mapp 2005;25:308–16. [PubMed: 15834863]
56. Lowe MJ, Horenstein C, Hirsch JG, et al. Functional pathway-defined MRI diffusion measures reveal increased transverse diffusivity of water in multiple sclerosis. Neuroimage 2006;32:1127–33. [PubMed: 16798013]
57. Ogawa S, Lee TE, Kay AR, Tank DW. Brain magnetic resonance imaging with contrast dependent on blood oxygenation. Proc Natl Acad Sci USA 1990;87:9868–72. [PubMed: 2124706]
58. Lee M, Reddy H, Johansen-Berg H, et al. The motor cortex shows adaptive functional changes to brain injury from multiple sclerosis. Ann Neurol 2000;47:606–13. [PubMed: 10805331]
59. Reddy H, Narayanan S, Arnoutelis R, et al. Evidence for adaptive functional changes in the cerebral cortex with axonal injury from multiple sclerosis. Brain 2000;123:2314–20. [PubMed: 11050031]
60. Buckle GJ. Functional magnetic resonance imaging and multiple sclerosis: the evidence for neuronal plasticity. J Neuroimaging 2005;15:S82–93.
61. Frohman EM, Costello F, Zivadinov R, et al. Optical coherence tomography in multiple sclerosis. Lancet Neurol 2006;5:853–63. [PubMed: 16987732]
62. Ko TH, Fujimoto JG, Duker JS, et al. Comparison of ultrahigh- and standard-resolution optical coherence tomography for imaging macular hole pathology and repair. Ophthalmology 2004;112:1922–35. [PubMed: 16183127]
63. Parisi V, Manni G, Spadaro M, et al. Correlation between morphological and functional retinal impairment in multiple sclerosis patients. Invest Ophthalomol Vis Sci 1999;40:2520–7.
64. Fisher JB, Jacobs DA, Markowitz CE, et al. Relation of visual function to retinal nerve fiber layer thickness in multiple sclerosis. Ophthalmology 2006;113:324–32. [PubMed: 16406539]
65. Costello F, Coupland S, Hodge W, et al. Quantifying axonal loss after optic neuritis with optical coherence tomography. Ann Neurol 2006;59:963–9. [PubMed: 16718705]
66. Pulicken M, Gordon-Lipkin E, Balcer LJ, et al. Optical coherence tomography and disease subtype in multiple sclerosis. Neurology 2007;69:2085–92. [PubMed: 18040015]
67. Gordon-Lipkin E, Chodkowski B, Reich DS, et al. Retinal nerve fiber layer is associated with brain atrophy in multiple sclerosis. Neurology 2007;69:1603–9. [PubMed: 17938370]
68. Levenson, MD.; Kano, SS. Introduction to nonlinear laser spectroscopy. San Diego: Academic Press; 1988.

69. Li L, Wang H, Cheng JX. Quantitative coherent anti-Stokes Raman scattering imaging of lipid distribution in co-existing domains. Biophys J 2005;89:3480–90. [PubMed: 16126824]
70. Potma EO, de Boeij WP, van Haastert PJM, Wiersma DA. Real-time visualization of intracellular hydrodynamics in single living cells. Proc Natl Acad Sci USA 2001;98:1577–82. [PubMed: 11171993]
71. Zumbusch A, Holtom GR, Xie XS. Three-dimensional vibrational imaging by coherent anti-Stokes Raman scattering. Phys Rev Lett 1999;82:4142–5.
72. Cheng JX, Volkmer A, Book LD, Xie XS. An epi-detected coherent anti-Stokes Raman scattering (E-CARS) microscope with high spectral resolution and high sensitivity. J Phys Chem B 2001;105:1277–80.
73. Ganikhanov F, Carrasco S, Xie XS, et al. Broadly tunable dual-wavelength light source for coherent anti-Stokes Raman scattering microscopy. Opt Lett 2006;31:1292–4. [PubMed: 16642089]
74. Burkacky O, Zumbusch A, Brackmann C, Enejder A. Dual-pump coherent anti-Stokes Raman scattering microscopy. Opt Lett 2006;31:3656–8. [PubMed: 17130935]
75. Cheng JX, Jia YK, Zheng G, Xie XS. Laser-scanning coherent anti-Stokes Raman scattering microscopy and applications to cell biology. Biophys J 2002;83:502–9. [PubMed: 12080137]
76. Evans CL, Potma EO, Puoris'haag M, Côté D, et al. Chemical imaging of tissue in vivo with video-rate coherent anti-Stokes Raman scattering microscopy. Proc Natl Acad Sci USA 2005;102:16807–12. [PubMed: 16263923]
77. Huff TB, Cheng JX. In vivo coherent anti-Stokes Raman scattering imaging of sciatic nerve tissue. J Microsc 2007;225:175–82. [PubMed: 17359252]
78. Stewart WA, MacKay AL, Whittall KP, et al. Spin–spin relaxation in experimental allergic encephalomyelitis. Analysis of CPMG data using a non-linear least squares method and linear inverse theory. Magn Reson Med 1993;29:767–75. [PubMed: 8350719]
79. Morell, P.; Quarles, RH. Myelin formation, structure, and biochemistry. In: Siegel, GJ.; Agranoff, BW.; Alberts, RW.; Molinoff, PB., editors. Basic neurochemistry: molecular, cellular, and medical aspects. Vol. 5. Lippincott Williams & Wilkins; Philadelphia: 1999.
80. Regenold WT, Phatak P, Marano CM, et al. Myelin staining of deep white matter in the dorsolateral prefrontal cortex in schizophrenia, bipolar disorder, and unipolar major depression. Psychiatry Res 2007;151:179–88. [PubMed: 17433451]
81. Wright SJ, Centonze VE, Stricker SA, et al. Introduction to confocal microscopy and three-dimensional reconstruction. Methods Cell Biol 1993;38:1–45. [PubMed: 8246779]
82. Fu Y, Wang HF, Shi RY, Cheng JX. Second harmonic and sum frequency generation imaging of fibrous astroglial filaments in ex vivo spinal tissues. Biophys J 2007;92:3251–9. [PubMed: 17293404]
83. Wang H, Huff TB, Fu Y, et al. Increasing the imaging depth of coherent anti-Stokes Raman scattering microscopy with a miniature microscope objective. Opt Lett 2007;32:2212–4. [PubMed: 17671587]

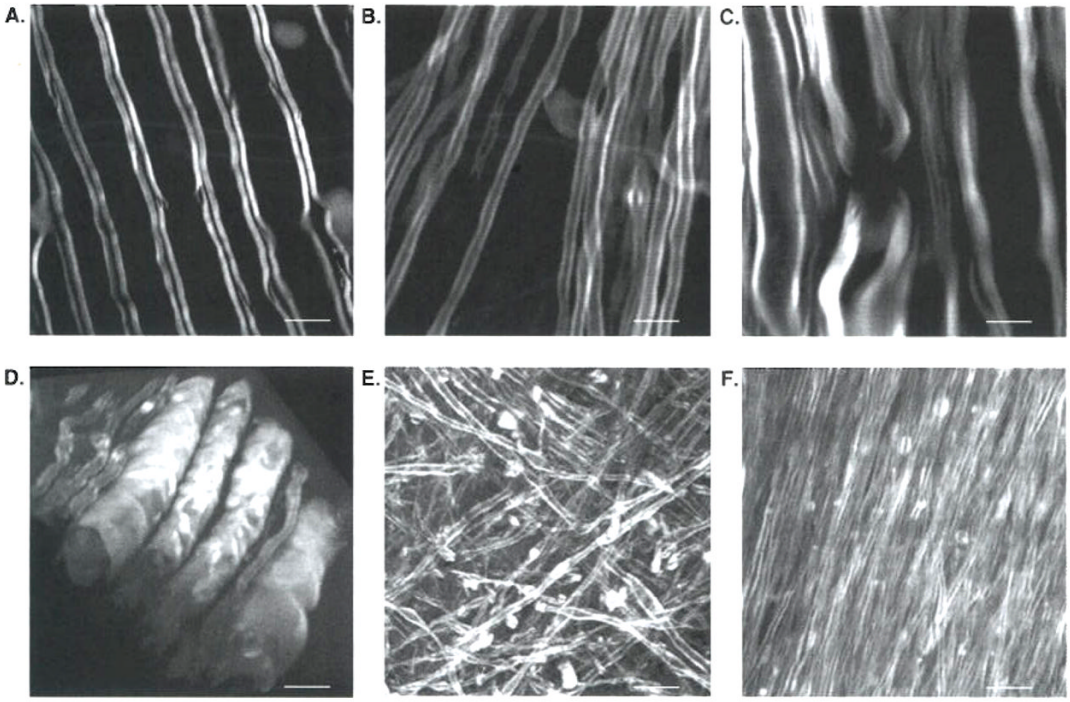

Figure 1. Coherent anti-Stokes Raman scattering (CARS) images of myelin fibers in ex *vivo* guinea-pig spinal cord and brain

A. Parallel myelin fibers were observed in spinal cord tissues. **B.** In brain, single myelinated axon was observed. **C.** With submicron resolution, a node of Ranvier flanked by paranodal myelin was observed by CARS microscopy, **D.** Three-dimensional reconstruction of myelinated fibers in spinal cord. **E.** Z stacks of CARS images in brain cortex showing myelinated axons in random orientations. **F.** Z stacks of CARS images in brain corpus callosum showing tightly packed axonal bundles. For **A, C – F,** bar = 10 μm. For **B,** bar = 5 μm.

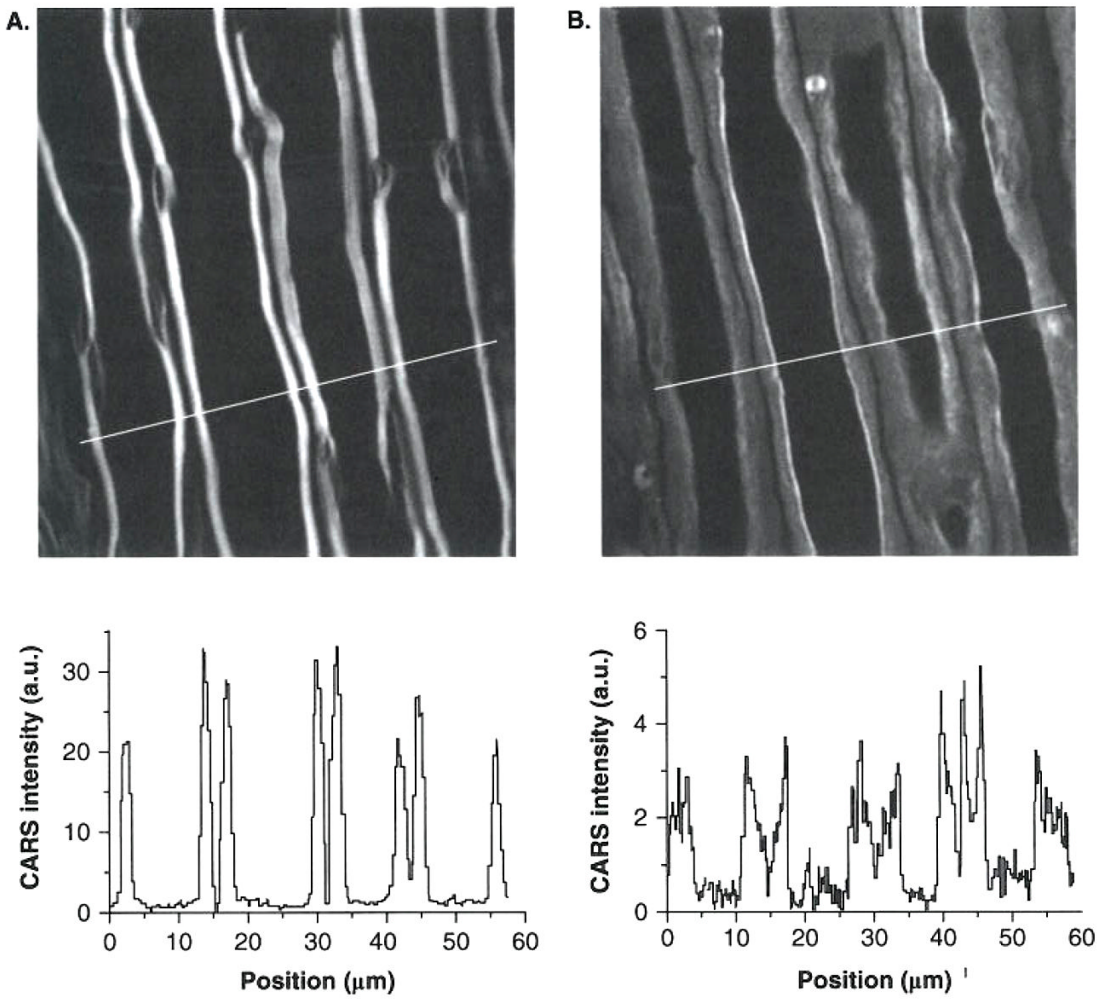

Figure 2. Real-time coherent anti-Stokes Raman scattering (CARS) imaging of demyelination processes induced by lyso-PtdCho

A. CARS image of normal myelin sheath wrapping four parallel axons. **B**. CARS image of partially swollen myelin sheath acquired at 31 min alter incubation of the tissue in 100 mg/ml lyso-PtdCho solution. Below **A** and **B** are CARS intensity profiles of normal and swollen myelin fibers. Note the decrease of CARS intensity in the swollen region.

Table 1

Summary of information provided by NMR techniques.

Methods	Information about MS lesions
MRI	T1 hypointense lesions (black holes) reflect chronic severe tissue pathology including axonal loss
	T2 hyperintense lesions provide total number and volume of disease lesions including reversible and irreversible pathologies
	T1 gadolinium enhancing lesions detect blood-brain barrier leakage and inflammatory disturbances
MRS	Decreased NAA levels reflect axonal damage. Whole brain NAA level may be a reliable measure of total disease burden in MS
MTI	Severe tissue damage associated with demyelination is detected. Focal changes in MTI precede findings in conventional MRI
DWI and DTI	Demyelination and axonal loss in white matter are detected. Subtle changes in normal appearing white matter can be seen. Significant correlations are obtained between findings and clinical manifestations
fMRI	Neural activity in response to tissue injury in MS is measured. Increased activity in fMRI compared with control suggests functional reorganization

DTI: Diffusion tensor imaging; DWI: Diffusion weighted imaging; fMRI: Functional MRI; MRS: Magnetic resonance spectroscopy; MS: Multiple sclerosis; MTI: Magnetization transfer imaging; NAA: *N*-acetyl aspartate.

Table 2

Comparison of MRI, optical coherence tomography (OCT) and coherent anti-Stokes Raman scattering (CARS).

	MRI	OCT	CARS microscopy
Contrast mechanisms	^{1}H nuclei magnetic resonance	Backreflection of photons	C–H vibration
Resolution			
Lateral	0.1~1 mm	15 ~20 μm	~0.3 μm
Axial	1 ~ 3 mm	3 ~ 10 μm	~ 0.7 μm
Penetration depth	Whole brain	1 ~3 mm	~ 100 μm
Imaging speed	10 min ~ 1 h	200 ms	50 ms ~ 1 s
Field of view	4 ~ 28 cm	6 mm	200 ~ 700 μm
Current applications	MS patients	Eyes in MS patients	Tissue and animal

MS: Multiple sclerosis.